A Mechanism for P-Glycoprotein-Mediated Apoptosis As Revealed by Verapamil Hypersensitivity

Joel Karwatsky, Maximilian C. Lincoln, and Elias Georges*

Institute of Parasitology, McGill University, Macdonald Campus, Ste-Anne de Bellevue, Quebec H9X 3V9, Canada

Received January 25, 2003; Revised Manuscript Received August 18, 2003

ABSTRACT: Selection of tumor cell lines with anticancer drugs has led to the appearance of multidrug-resistant (MDR) subclones with P-glycoprotein 1 (P-gp1) expression. These cells are cross-resistant to several structurally and functionally dissimilar drugs. Interestingly, in the process of gaining resistance, MDR cells become hypersensitive or collaterally sensitive to membrane-active agents, such as calcium channel blockers, steroids, and local anaesthetics. In this report, hypersensitivity to the calcium channel blocker, verapamil, was analyzed in sensitive and resistant CHO cell lines. Our results show that treatment with verapamil preferentially induced apoptosis in MDR cells compared to drug-sensitive cells. This effect was independent of p53 activity and could be inhibited by overexpression of the Bcl-2 gene. The induction of apoptosis by verapamil had a biphasic trend in which maximum cell death occurred at 10 μM, followed by improved cell survival at higher concentrations (50 μM). We correlated this effect to a similar biphasic trend in P-gp1 ATPase activation by verapamil in which low concentrations of verapamil (10 μM) activated ATPase, followed by inhibition at higher concentrations. To confirm the relationship between apoptosis and ATPase activity, we used two inhibitors of P-gp1 ATPase, PSC 833 and ivermectin. These ATPase inhibitors reduced hypersensitivity to verapamil in MDR cells. In addition, low concentrations of verapamil resulted in the production of reactive oxygen species (ROS) in MDR cells. Taken together, these results show that apoptosis was preferentially induced by P-gp1 expressing cells exposed to verapamil, an effect that was mediated by ROS, produced in response the high ATP demand by P-gp1.

The rise of multidrug-resistant (MDR)[1] tumor subclones has long been recognized as a major obstacle in clinical anticancer treatment. Although several mechanisms of drug resistance exist, the 170-kDa P-glycoprotein 1 (P-gp1) is one of the best-characterized causes of multidrug resistance. P-gp1 is an ATP-binding cassette (ABC) protein that causes energy-dependent efflux of many unrelated hydrophobic drugs from cancer cells (*1*, *2*). Accordingly, much emphasis has been placed on identifying chemosensitizers, also called reversing agents. These are nontoxic compounds that interact with P-gp1 and inhibit its drug efflux function, thereby preventing drug resistance (*3*). Ironically, some MDR cells develop hypersensitivity to previously harmless drugs and chemosensitizers (*4*). Hypersensitivity or "collateral sensitivity" in MDR cells has been observed with calcium channel blockers (*5*, *6*), steroids (*7*), nonionic detergents, and local anaesthetics (*4*, *8*). The calcium channel blocker, verapamil, is a classic chemosensitizer (*9*) that causes hypersensitivity in several MDR cell lines (*5*, *6*, *10*). The MDR reversal effect of verapamil on P-gp1 is apparently independent of its ability to block calcium channels (*5*, *11*).

In addition to reversing drug resistance, verapamil induces a high level of ATP hydrolysis by P-gp1 (*12*). Several reports have shown that the ATPase activity of P-gp1 is important for drug transport, although the mechanism by which ATP hydrolysis is coupled to drug transport is still unclear (*13*−*15*). Unlike other ABC proteins, P-gp1 exhibits a high level of basal ATPase activity in the absence of drugs. The basal activity may be caused by transporting endogenous lipids or hydrophobic peptides (*16*, *17*). ATPase activity that is uncoupled from substrate transport may also contribute to the basal activity (*18*). The compounds that affect P-gp1 ATPase activity are classified into three categories. Class I compounds stimulate ATPase activity at low concentrations but inhibit activity at high concentrations. Class II compounds enhance ATPase activity as their concentration increases. Class III compounds inhibit basal and drug-stimulated ATPase activity (*12*, *18*−*20*). Verapamil is a class I agent that increases ATPase to very high levels before inhibiting activity (*20*). Other chemosensitizers, such as cyclosporin A and the cyclosporin derivative PSC 833, are very effective class III ATPase inhibitors.

We report that the P-gp1 overexpressing CHO cell lines, CH^RC5 and CH^R30, underwent heightened levels of apoptosis upon treatment with low concentrations of verapamil relative to the parental AUXB1 and revertant I10 cells. Cell death was inhibited by the stable transfection of CH^RC5 with Bcl-2 and occurred independently of p53 activation. Verapamil-

* Corresponding author. Tel.: (514) 398-8137. Fax: (514) 398-7857. E-mail: Elias.Georges@McGill.ca.

[1] Abbreviations: CDDP, cisplatin; CX, cycloheximide; MDR, multidrug-resistant; P-gp1, P-glycoprotein 1; SDS−PAGE, sodium dodecyl sulfate−polyacrylamide gel electrophoresis; ROS, reactive oxygen species; SDZ PSC 833, PSC 833; ETC, electron transport chain.

10.1021/bi034149+ CCC: $25.00
Published on Web 10/03/2003

induced apoptosis was correlated to increased P-gp1 ATPase activation and elevated levels of reactive oxygen species (ROS). We used the ATPase inhibitors PSC 833 and ivermectin to inhibit verapamil-induced ROS production, thereby reducing verapamil hypersensitivity. These observations suggest that the apoptotic pathway resulting from hypersensitivity to verapamil is mediated by ROS production via elevated oxidative phosphorylation.

EXPERIMENTAL PROCEDURES

Reagents. All chemicals were of analytical grade and purchased from Sigma (Oakville, Ontario, Canada). PSC 833 was provided by Novartis (East Hanover, NJ). The Rc/RSV, LipofectAMINE, and G418 sulfate were purchased from Gibco-BRL (Burlington, Ontario, Canada). The ATPLite luminescence ATP detection system was obtained from PerkinElmer Life Sciences (Woodbridge, Ontario, Canada). Monoclonal anti-Bcl-2 (Ab-3) antibody was purchased from Calbiochem (San Diego, CA), and polyclonal anti-Bax (N-20) antibody was purchased from Santa Cruz Biotechnology (Santa Cruz, CA).

Cell Culture Conditions and Cell Lines. The Chinese hamster ovary (CHO) cell lines AUXB1, CH^RC5, CH^R30, and I10 were kindly provided by Dr. V. Ling of the British Columbia Cancer Institute, Vancouver, Canada, and grown in alpha-minimal essential medium (α-MEM) supplemented with 10% foetal calf serum (FCS) at 37 °C in the presence of 5% CO_2. CH^RC5 was derived by clonal stepwise selection from the drug-sensitive parental line, AUXB1 (*21*). CH^R30 was derived from CH^RC5 by stepwise selection with colchicine. I10 is a drug-sensitive revertant cell line derived in a single step from CH^RC5 (*22*).

Dose−Response Assays. For dose−response assays, cells were added to 24-well plates at a concentration of 2000 cells per well (to produce single cell colonies) and incubated with α-MEM with 10% FCS. After 24 h of growth, verapamil was added to the medium. When the ATPase inhibitors PSC 833 and ivermectin were used concurrently with verapamil, cells were preincubated with inhibitor for 30 min before the addition of verapamil. Either the cells were incubated in verapamil for 24 h, after which the cells were washed and new medium was added, or the cells were grown in verapamil continuously for 5 days. After a total of 6 days, surviving colonies were counted, stained with methylene blue dye, air-dried, and solubilized in 0.1% (v/v) SDS/PBS. The absorbance of the resulting solution was determined colorimetrically at 510 nm in a multiplate photospectrometer (Dynatech Laboratories, MR5000). Cell viability is expressed as a percentage of untreated control cells. Cell viability results represent the average of at least four independent experiments done in triplicate.

DNA Fragmentation Assay To Measure Apoptosis. AUXB1 and CH^RC5 cells were treated with verapamil, cisplatin (CDDP), the racemeric isomer (*R*)-(+)-verapamil, or cycloheximide (CX). Fragmented genomic DNA was quantified 24 h after treatment as previously described (*23*). Briefly, adherent and nonadherent cells were pooled, washed three times in phosphate-buffered saline (PBS), and resuspended in buffer A (0.15 M NaCl, 10 mM Tris pH 7.4, 2 mM $MgCl_2$, and 1 mM dithiothreitol). Nonidet P-40 (0.5% v/v) was added to the mixture, and the samples were left for 30 min on ice. After centrifugation at 16000*g* for 5 min, the supernatant was discarded and the resulting pellet resuspended in buffer B (0.35 M NaCl, 10 mM Tris pH 7.4, 2 mM $MgCl_2$, and 1 mM dithiothreitol) and again left on ice for 30 min. Following a second centrifugation step at 16000*g*, the supernatant was removed and extracted with a phenol−chloroform solution. The resulting aqueous solution, containing fragmented genomic DNA, was precipitated with an equal volume of ethanol. The DNA pellet was resuspended in Tris−EDTA and treated with DNAase-free RNAase A for 30 min at 37 °C prior to electrophoresis on a 1% agarose gel.

Flow Cytometry Analysis To Assess Apoptosis. AUXB1 and CH^RC5 cells were treated with varying concentrations of CDDP, verapamil, or (*R*)-(+)-verapamil for 24 h and then harvested and washed with PBS. After centrifugation, all samples were resuspended dropwise with vortexing in 2 mL of 70% ice-cold ethanol, followed by a 60-min incubation at 4 °C. The cells were washed once with PBS and then incubated in PBS containing RNAase A (1 μg/mL) at 37 °C for 10 min. After centrifugation, the samples were resuspended in PBS with propidium iodide (PI, 50 μg/mL) and incubated overnight in the dark at 4 °C. Fluorescence of PI-stained nuclei was read using a FACScan flow cytometer (Becton Dickinson, Mountain View, CA). The percentage of cells undergoing apoptosis was obtained through comparison of the relative proportions of diploid and subdiploid (apoptotic) nuclear DNA.

CAT Assay To Measure p53 Activity. p53 activity was measured by transfection with a PG-13 CAT construct, containing 13 repeats of a ribosomal gene cluster sequence previously shown to interact with p53 as a promoter for the chloramphenicol acetyltransferase (CAT) gene (*24*). Briefly, co-transfections of AUXB1 and CH^RC5 cells with 5 μg of PG-13 CAT construct and 2 μg of RSV-galactosidase plasmid were carried out according to the manufacturer's instructions using LipofectAMINE. After 24 h, the plates were treated with verapamil (10−50 μM) or 15 s of UV light (875 mJ/m^2). After another 48 h, all samples were harvested in CAT buffer A (40 mM Tris pH 7.5, 150 mM NaCl, and l mM EDTA) and subjected to three repetitions of a freeze−thaw cycle prior to lysis. Samples were normalized with a galactosidase assay and incubated at 65 °C for 10 min. After centrifugation, the supernatants were incubated with 5 μL of CAT buffer B (33.3 mg/mL N-butyril CoA, 5 μL of 50 Ci/mmol [^{14}C]chloramphenicol, and 25 mM Tris pH 7.5). After a 2 h incubation at 37 °C, samples were extracted with ethyl acetate, separated by thin-layer chromatography (TLC), and subjected to autoradiography. TLC plates containing both substrate and the mono- and diacetylated products were resuspended in scintillation cocktail. CAT activity was measured in counts per minute and expressed as a percentage of the UV control.

Western Blot of Endogenous P-gp1, Bax, and Bcl-2 Protein Levels. Western blot analysis was performed on 20−200 μg of total cell lysate and resolved on 10% acrylamide gels using the Laemmli gel system (*25*). Proteins separated by SDS−PAGE were then transferred to nitrocellulose membrane (*26*). The membranes were probed with monoclonal anti-P-gp1 (C-219), monoclonal anti-Bcl-2 (Ab-3), or polyclonal anti-Bax (N-20) antibodies.

Transfection of Bcl-2 into CH^{R}C5 Cells. CH^{R}C5 cells were seeded at 0.5×10^6 cells per well in 60-mm plates and transfected with an Rc/RSV vector containing a full-length gene of human Bcl-2 cDNA (generously provided by Dr. G. Shore, Department of Biochemistry, McGill University) according to the manufacturer's instructions using LipofectAMINE. Several colonies were isolated in the presence of 1 mg/mL of G418 sulfate. Single-cell clones from G418-resistant colonies were immediately selected in 96-well plates and cultured continuously in G418. The expression of Bcl-2 in CH^{R}C5 transfectants (CH^{R}C5/Bcl-2) was determined by Western blot analysis using the monoclonal anti-Bcl-2 antibody as described above.

Viability of VRP-Treated AUXB1, CH^{R}C5, and CH^{R}C5/Bcl-2 Cells. All three cell lines were seeded at 0.5×10^6 cells in 60-mm plates and treated after 24 h with 10 μM verapamil or 50 μM CDDP, or left untreated. Forty-eight hours after treatment, cells were harvested and resuspended in equal volumes of PBS, and the number of viable Trypan blue-stained cells was counted for each sample. Cell viability is expressed as a percentage of untreated controls. Cell viability results represent the average of at least four independent experiments done in triplicate.

Hoechst Dye Staining for Apoptosis. AUXB1 and CH^{R}C5 cells were incubated with and without 10 μM verapamil for 36 h. Hoechst 33258 dye was then added at 1 μg/mL to the media. After a 10-min incubation at 37 °C, the cells were observed under UV light for signs of apoptosis. Photographs were taken at 2000× magnification (Nikon, Eclipse TE200, Montreal, Quebec, Canada).

Isolation of Purified Plasma Membranes. All steps were preformed at 4 °C. AUXB1 and CH^{R}C5 cells were washed with PBS before being resuspended in 10 mL of lysis buffer (10 mM HEPES−Tris pH 7.4, 5 mM EDTA, 5 mM EGTA, and 2 mM dithiothreitol) containing protease inhibitors (2 mM PMSF, 10 μg/mL leupeptin, and 10 μg/mL pepstatin). Cells were lysed in a glass homogenizer (Kontes, Vineland, NJ). Nuclei were sedimented by centrifugation at 300*g* for 10 min; mitochondria were then removed by centrifugation at 400*g* for 10 min. A final centrifugation at 45000*g* for 60 min was used to sediment the plasma membrane fraction. The pellet was resuspended in 1 mL of the lysis buffer and homogenized by aspiration 10 times through a 27-gauge syringe. The membrane samples were stored at −80 °C.

P-gp1 ATPase Activity Assay. The P-gp1 ATPase activity was determined by quantifying the release of inorganic phosphate from ATP according to Litman et al. (*20*). AUXB1 and CH^{R}C5 plasma membrane samples were diluted to 20 μg/mL in ice-cold ATPase assay medium (3 mM ATP, 100 mM KCl, 10 mM $MgCl_2$, 4 mM dithiothreitol, 100 mM Tris pH 8.0, 4 mM EGTA, 2 mM ouabain, and 10 mM NaN_3). Each series of experiments was conducted in a 96-well plate, with reaction volumes of 50 μL/well corresponding to 1 μg of protein/well. Incubation with verapamil was started by transferring the plate from ice to 37 °C for 1 h, and terminated by the addition of 200 μL of ice-cold stopping medium (0.2% ammonium molybdate (w/v), 1.3% sulfuric acid (v/v), 0.9% SDS (w/v), 2.3% trichloroacetic acid (w/v), and 1% ascorbic acid (w/v)) to each well. After a 75-min incubation at room temperature, the released phosphate was quantified colorimetrically in a microplate reader (Dynatech Laboratories, MR5000) at 630 nm. Plasma membranes were incubated with the ATPase inhibitors PSC 833 and ivermectin for 30 min before the addition of verapamil. The results for P-gp1 ATPase activity were fitted using the following equation (*20*):

$$V_{(s)} = \frac{K_1K_2V_0 + K_2V_1S + V_2S^2}{K_1K_2 + K_2S + S^2}$$

where $V_{(s)}$ is the ATPase activity as a function of substrate concentration, V_0 is the basal activity, V_1 is the maximal enzyme activity, K_1 is the substrate concentration that produces half the maximal increment in ATPase activity, V_2 is the activity at infinite concentration of the modulator, and K_2 is the substrate concentration that produces half-maximal reduction in ATPase activity from the value V_1. Each condition was performed with three to six replicates a minimum of three times.

MTT Test for Superoxide Production. 3-(4,5-Dimethylthiazol-2-yl)-2,5-diphenyltetrazolium bromide (MTT) is a tetrazolium dye that can be reduced to its colored formazan by the ROS, superoxide (O_2^-) (*27*). MTT was used to determine ROS production of AUXB1 and CH^{R}C5 cells. AUXB1 and CH^{R}C5 cells were seeded in 24-well plates at 1.5×10^5 and 1×10^5 cells/well, respectively. After 24 h, a solution containing verapamil was added to cells at final concentrations of 10, 25, and 75 μM, with 0.5 mg/mL MTT in PBS. The cells were incubated at 37 °C, and readings were taken after 1.5 h. The media mixture was removed by aspiration, and 250 μL of 10% Triton-X100 in 0.01 N HCl was added to each well. The samples were then incubated at 37 °C until the reduced MTT was completely dissolved in solution. Samples were removed, and their absorbance was quantified colorimetrically in a microplate reader at 570 nm. The amount of superoxide produced was determined relative to the OD of untreated controls. The status of cell survival was examined by Trypan blue staining to confirm that 1.5 h of exposure to verapamil did not cause cell death.

Measurement of Total GSH. AUXB1 and CH^{R}C5 cells were seeded in 25 cm^2 flasks at a density of 6×10^5 and 4×10^5 cells/well, respectively. After 48 h, the cells were washed three times with ice-cold PBS before scraping. The cells were then collected in ice-cold PBS and pelleted by centrifugation at 150*g* for 5 min at 4 °C. The cells were resuspended in 100 μL of 10 mM HCl and lysed by freeze−thawing in liquid nitrogen three times. After lysis, the sample was pelleted at 6000*g* for 5 min at 4 °C. Subsequently, 100 μL of supernatant was added to 400 μL of picric acid, vortexed, and centrifuged at 16000*g* for 5 min at 4 °C and the supernatant was collected. In a cuvette, 700 μL of daily buffer (0.3 mM NADPH, 143 mM Na_2HPO_4, 6.3 mM Na_4−EDTA, pH 7.5), 100 μL of DTNB (6 mM 5,5′-dithiobis-2-nitrobenzoic acid), 143 mM Na_2HPO_4, 6.3 mM Na_4−EDTA, pH 7.5), and 150 μL of water was warmed to 30 °C for 12−15 min. After warming, 40 μL of sample or standard (GSH) and 10 μL of GSSG reductase were added to the cuvette and mixed. The formation of yellow TNB was followed continuously on a spectrometer at 412 nm while the slope remained constant. The slope of each sample was compared to a control to determine the percent change in GSH. The values obtained were the averages of three experiments done in triplicate.

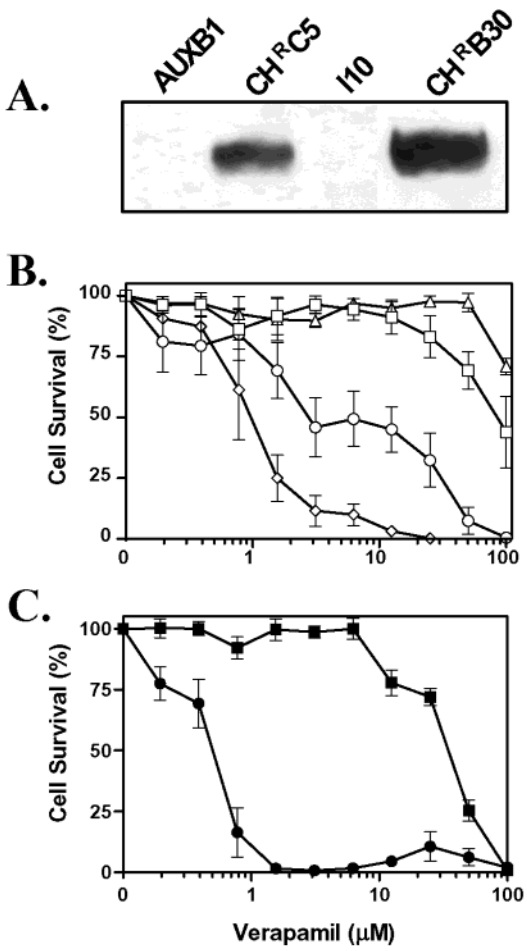

FIGURE 1: Western blot and verapamil dose−response assays for sensitive and multidrug resistant CHO cells. (A) The relative amount of P-gp1 protein is shown by Western blot using the P-gp1 specific mAb, C-219, in the parental AUXB1 cells, the multidrug-resistant CH^{R}C5 and CH^{R}B30 cells, and I10 (drug-sensitive revertant derived from CH^{R}C5). (B) AUXB1 (white squares), CH^{R}C5 (white circles), CH^{R}B30 (white diamonds), and I10 (white triangles) were exposed to increasing concentrations of verapamil for 24 h, followed by 4 days of growth in drug-free conditions. The surviving colonies were stained with methylene blue and quantified by spectrophotometry. (C) AUXB1 (black squares) and CH^{R}C5 (black circles) were exposed to increasing verapamil concentrations for 5 days and survival was quantified as in (B).

Measurement of Total Cellular ATP. AUXB1 and CH^R-C5 cells were seeded in black 96-well plates at a density of 2×10^4 and 2.5×10^4 cells/well, respectively. After 24 h of growth, the cells were exposed to verapamil alone, or in conjunction with a 30-min pretreatment of 2 μM PSC 833 or 4 μM invermectin. The ATPlite luminescence ATP detection assay system was used to monitor ATP levels. This monitoring system is based on firefly (*Photinus pyralis*) luciferase.

RESULTS

Characterization of Hypersensitivity to Verapamil in CHO Cell Lines. Hypersensitivity to verapamil has been previously demonstrated in several MDR cell lines that overexpress P-gp1 (*4*−*6*). To explore the mechanisms involved in verapamil sensitivity, it was important to confirm this effect in cells expressing increasing levels of P-gp1 (Figure 1A). Western blot analysis of the four CHO cells lines AUXB1, CH^{R}C5, I10, and CH^{R}B30 with the monoclonal antibody C-219 confirmed that AUXB1 and I10 have undetectable levels of P-gp1. CH^{R}B30 had higher P-gp1 levels than CH^R-C5. Clonal cell viability assays were conducted by exposing the four CHO cell lines with different levels of P-gp1 expression to verapamil for 24 h (Figure 1B). AUXB1 was relatively unaffected by verapamil up to 50 μM, whereas verapamil reduced the survival of CH^{R}C5 by 40% at concentrations as low as 2 μM. Furthermore, the more highly resistant CH^{R}B30 cell line was exceptionally sensitive to verapamil ($IC_{50} < 1$ μM). The disparity of survival between the different cell lines was most obvious at roughly 10 μM verapamil. AUXB1 was unaffected at this concentration, whereas CH^{R}C5 and CH^{R}B30 survival was reduced to approximately 50% and 2%, respectively. The survival of non-MDR I10 cells was the least affected by verapamil toxicity. These results suggest that hypersensitivity to verapamil in MDR CHO cells correlates with P-gp1 expression. Remarkably, we repeatedly observed an interesting trend in the survival curve of CH^{R}C5 when cells were exposed to verapamil for 5 days (Figure 1C) as opposed to 24 h (Figure 1B). CH^{R}C5 had consistently poor survival between 1 and 10 μM verapamil, followed by a moderate recovery above this concentration. In particular, CH^{R}C5 survival was several-fold higher at 50 μM verapamil than at 1.5 μM. This observation indicated that CH^{R}C5 hypersensitivity to verapamil was more pronounced at low concentrations.

Hypersensitivity to Verapamil and Apoptosis. To determine the mechanism that causes hypersensitivity, it was of interest to establish whether verapamil sensitivity was mediated by apoptosis or necrosis. For this purpose, DNA fragmentation was assessed in AUXB1 and CH^{R}C5 (Figure 2A). Treatment of both cell lines with increasing concentrations of verapamil (10−50 μM) resulted in the appearance of an oligonucleosomal ladder characteristic of apoptosis in CH^{R}C5 but not AUXB1 cells. DNA laddering of CH^{R}C5 decreased in a dose-dependent manner up to 50 μM, consistent with increased survival seen at higher verapamil concentrations (Figure 1C). Cisplatin (CDDP), known to induce interstrand bulky adducts in DNA, was used as a positive control for apoptosis (*28*) in both AUXB1 and CH^{R}C5 cells (Figure 2A).

Since apoptosis has been shown to require protein synthesis in some instances (*28*), the inhibition of protein synthesis by cycloheximide (CX) revealed a decrease in the levels of verapamil-induced apoptosis in CH^{R}C5 cells. A marked reduction in DNA laddering was apparent in verapamil- or CDDP-treated CH^{R}C5 cells preincubated with CX (1 μg/mL) for 30−60 min. Therefore, both verapamil- and CDDP-induced apoptosis in CH^{R}C5 cells required protein synthesis and can be blocked with CX. Similar results were also present for CDDP-treated AUXB1 cells preincubated with CX. To confirm the nature of cell death, the cellular nuclei were stained with Hoechst 33258. Representative photographs in Figure 2B show the staining of condensed chromatin in CH^{R}C5 cells exposed to 10 μM verapamil. AUXB1 cells that were exposed to verapamil show little or no apoptosis (Figure 2B). Moreover, FACScan analyses of propidium iodide-stained nuclei from AUXB1 and CH^{R}C5 cells treated with either verapamil or CDDP are shown in Figure 2C. The relative proportions of apoptotic, aneuploid cells are summarized in Figure 2C. Verapamil treatment preferentially induced an apoptotic, subdiploid peak in CH^R-

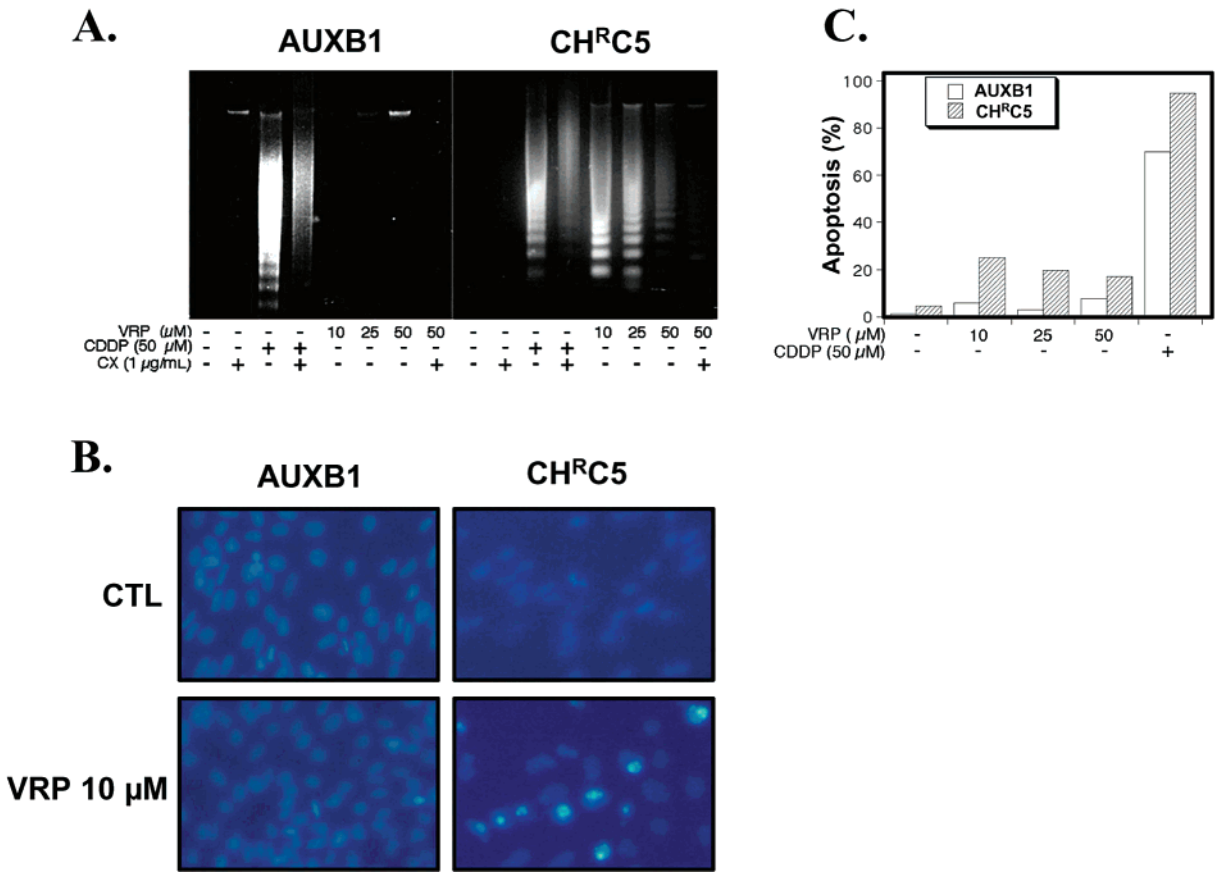

FIGURE 2: Analysis of apoptosis by DNA laddering, nuclear staining, and flow cytometry in AUXB1 and CH^{R}C5 cells in response to verapamil. (A) DNA fragmentation was measured in AUXB1 and CH^{R}C5 cells treated with increasing concentrations of verapamil (VRP). A 50 μM concentration of cisplatin (CDDP) was used as a positive control, and 1 mg/mL of cycloheximide (CX) was used to inhibit apoptosis. (B) Hoechst 33258 was added to determine the apoptotic state of AUXB1 and CH^{R}C5 cells grown with 10 μM verapamil and untreated. (C) Cells were treated for 24 h with the indicated concentrations of verapamil prior to quantification of apoptosis by flow cytometry. The cell number versus fluorescence is plotted for each treatment; concentrations for each drug appear in parentheses at the bottom of the graph.

C5 but not AUXB1 cells, while CDDP had a similar effect on both cell lines. Consistent with results from the DNA fragmentation assay of Figure 2A, CH^{R}C5 cells treated with verapamil showed a dose-dependent decrease in the number of aneuploid nuclei at concentrations above 10 μM. These results show that the cell death caused by verapamil in CH^R-C5 occurs by apoptosis alone. The highest levels of verapamil-induced apoptosis occurred at 10 μM. Again, the fact that the apoptotic effect of verapamil on CH^{R}C5 cells decreased at concentrations above 10 μM was consistently observed and supports the results of the cell survival assay in Figure 1C.

Previous studies have shown that verapamil hypersensitivity in MDR cells is independent of its calcium blocking activities since verapamil is unable to alter accumulation of [$^{45}Ca^{2+}$] from extracellular stores in AUXB1 or CH^{R}C5 cells (*5*, *29*). However, given the role of calcium levels in apoptosis, it was important to examine the effects of (*R*)-(+)-verapamil (a nonactive isomer of verapamil) on AUXB1 and CH^{R}C5 cells. Both DNA fragmentation and flow cytometry experiments showed that treatment of CH^{R}C5 cells with (*R*)-(+)-verapamil resulted in apoptotic levels comparable to those induced by racemic verapamil (data not shown). Therefore, the ability of verapamil to block calcium channels does not account for the apoptotic effect of the drug on CH^{R}C5 cells.

p53 Activity in Verapamil-Mediated Apoptosis. The tumor suppressor p53 can induce apoptosis in cells that have been incubated with DNA-damaging agents (*30*). Although verapamil has not previously been shown to be a DNA-damaging agent, it is known to phosphorylate protein kinase C, an activator of p53 (*31*, *32*). To determine if verapamil-induced apoptosis in CH^{R}C5 cells involves p53 activation, both AUXB1 and CH^{R}C5 cells were transiently transfected with the PG-13 construct, and CAT activity was measured in response to increasing concentrations of verapamil. Figure 3 shows relative CAT activities for both cell lines. A dose-dependent increase in p53-induced CAT activity was present upon verapamil treatment of AUXB1 drug-sensitive cells. In contrast, treatment with 10 and 25 μM verapamil caused a decrease in p53-induced CAT activity in CH^{R}C5 cells, although higher concentrations of verapamil (50 μM) led to a small increase in p53-induced CAT activity. As a positive control, a 15 s exposure of cells to UV light caused a large increase in p53 CAT activity in both cell lines. The discrepancy seen in PG-13 CAT activity between AUXB1 and CH^{R}C5 cells in the presence of low concentrations of verapamil may be a consequence of the differential uptake of the drug between the two cell lines as verapamil is effluxed by P-gp1 (*5*). Furthermore, p53 activation did not correspond with the apoptosis observed with verapamil treatment of AUXB1 or CH^{R}C5 cells (Figures 1 and 2).

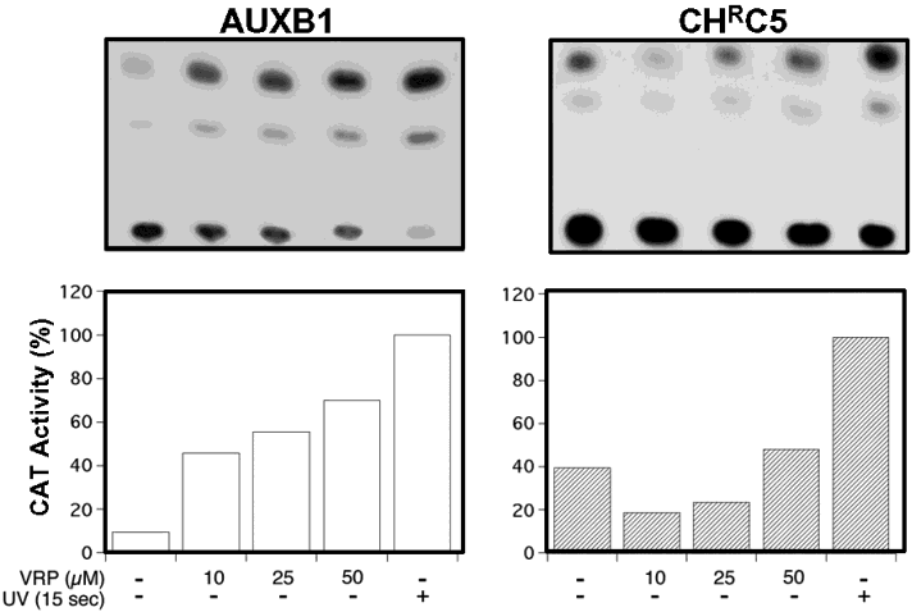

FIGURE 3: PG-13 CAT activity in AUXB1 and CHRC5 cells treated with varying concentrations of verapamil. CAT activity was measured in AUXB1 and CH^{R}C5 cells 48 h after incubation with verapamil (VRP) at 10, 25, or 50 μM, or 15 s exposure to UV light (as indicated below). The corresponding bar graph depicts CAT activity in both AUXB1 and CH^{R}C5 cells under these conditions. Enzyme activity was calculated by scraping the radioactive material from each assay and determining the percentage of product from the entire radioactive material in each case. Results appear as a percentage of the CAT activity in the UV treatment.

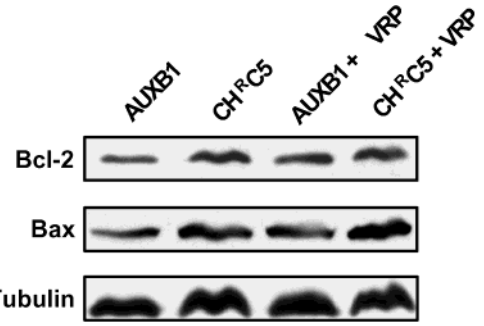

FIGURE 4: Endogenous Bcl-2 and Bax levels in AUXB1 and CH^{R}C5 cells. Cell lysates from verapamil (VRP)-treated (10 μM) or untreated AUXB1 and CH^{R}C5 cells were resolved by SDS−PAGE and transferred to nitrocellulose membrane. The nitrocellulose membrane was probed with anti-serum against Bcl-2 or Bax. A nonspecific reactive band migrating with a molecular mass of ~50 kDa served as control for loading.

Endogenous Bax and Bcl-2 Expression. To further characterize the apoptotic components of verapamil-sensitive CH^{R}C5 cells, we examined the levels of Bax and Bcl-2. Both proteins are involved in the control of apoptosis. Bcl-2 expression is associated with inhibition of apoptosis, while Bax stimulates apoptosis. Figure 4 shows a Western blot of cell lysates from AUXB1 and CH^{R}C5 treated and untreated with 10 μM verapamil, probed with anti-Bcl-2 or anti-Bax antibodies. Treatment with 10 μM verapamil did not result in an increase in Bax levels above untreated controls in either AUXB1 or CH^{R}C5 cells. In contrast, AUXB1 but not CH^{R}C5 cells showed a slight increase in Bcl-2 above control levels when treated with verapamil.

Overexpression of Bcl-2 in CH^{R}C5 and Inhibition of Verapamil Hypersensitivity. Bcl-2 exerts its principal effects through stabilizing mitochondria and preventing the release of cytochrome *c*. To further assess the pathway of verapamil-induced apoptosis, stable transfectants of CH^{R}C5 with full-length human-specific Bcl-2 cDNA were generated. The resulting clone, CH^{R}C5/Bcl-2, expressed vastly increased levels of human specific Bcl-2, as seen by Western blot analysis with a human-specific anti-Bcl-2 mAb (Figure 5A). CH^{R}C5/Bcl-2 cells treated for 48 h with 10 μM verapamil retained a heightened level of viability relative to CH^{R}C5 cells, as assessed by Trypan blue staining (Figure 5B). CDDP-treated CH^{R}C5/Bcl-2 cells similarly retained heightened cell viability relative to AUXB1 and CH^{R}C5 cells. To determine whether CH^{R}C5/Bcl-2 cells were protected from the toxicity of verapamil through suppression of apoptosis, a DNA fragmentation assay was carried out on AUXB1, CH^{R}C5, and CH^{R}C5/Bcl-2 cells treated for 24 h with either 10 μM verapamil or 50 μM CDDP (Figure 5C). No oligonucleosomal laddering was present in verapamil- or CDDP-treated samples of CH^{R}C5/Bcl-2 cells, demonstrating that apoptosis was diminished relative to CH^{R}C5 cells.

Inhibition of P-gp1 ATPase Activity and Reduced Hypersensitivity to Verapamil. The DNA laddering and FACScan experiments (Figure 2A,B) demonstrated the ability of verapamil to induce apoptosis. The cell survival experiments and apoptosis assays (Figures 1 and 2) indicated that the P-gp1-expressing cells were most sensitive to verapamil at about 10 μM, with improved survival at higher concentrations. In addition to inducing cell death in P-gp1-expressing cells, verapamil is also one of the most potent activators of P-gp1 ATPase activity (*20*). Verapamil stimulates ATPase activity at low concentrations but inhibits the activity at high concentrations. This prompted us to test the response of P-gp1 ATPase to verapamil in AUXB1 and CH^{R}C5 cells. Figure 6A shows a representative profile of P-gp1 ATPase activity in AUXB1 and CH^{R}C5 plasma membranes exposed to increasing amounts of verapamil. The increase and subsequent decrease of ATP hydrolysis in CH^{R}C5 cells paralleled the apoptotic profile of these cells (as seen in Figure 2). P-gp1 ATPase activity was not observed with AUXB1. Verapamil induced maximal ATPase activation at

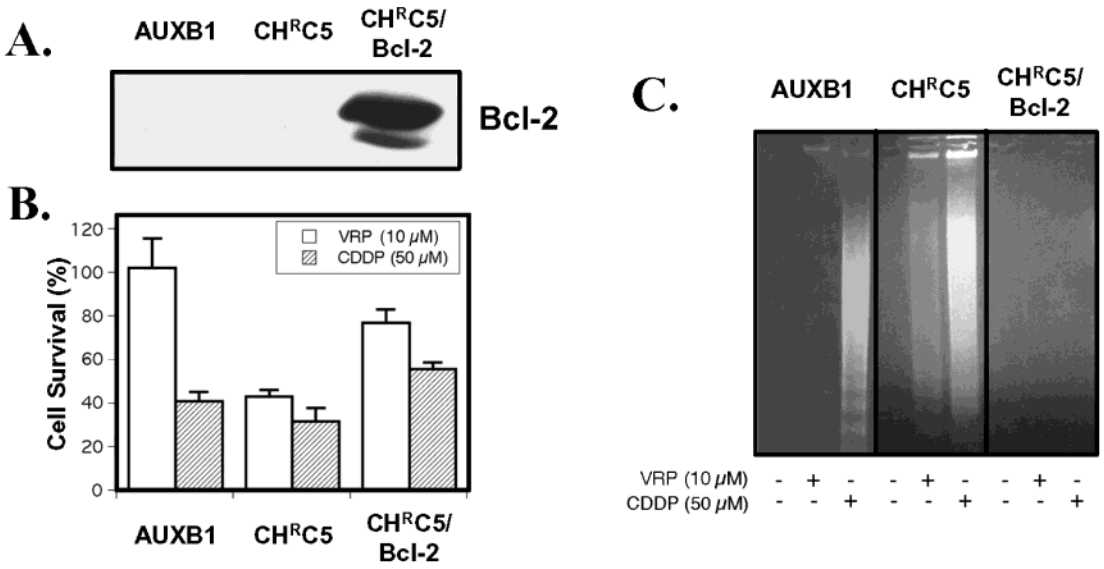

FIGURE 5: Effect of Bcl-2 overexpression on verapamil hypersensitivity in CH^{R}C5 cells. (A) Total cell lysates from AUXB1, CH^{R}C5, and CH^{R}C5/Bcl-2 cells were prepared for Western blotting and probed with human specific Bcl-2 mAb. (B,C) Cell viability and DNA laddering of AUXB1, CH^{R}C5, and CH^{R}C5/Bcl-2 cells following 48 h treatment with 10 μM verapamil (VRP) or 50 μM cisplatin (CDDP).

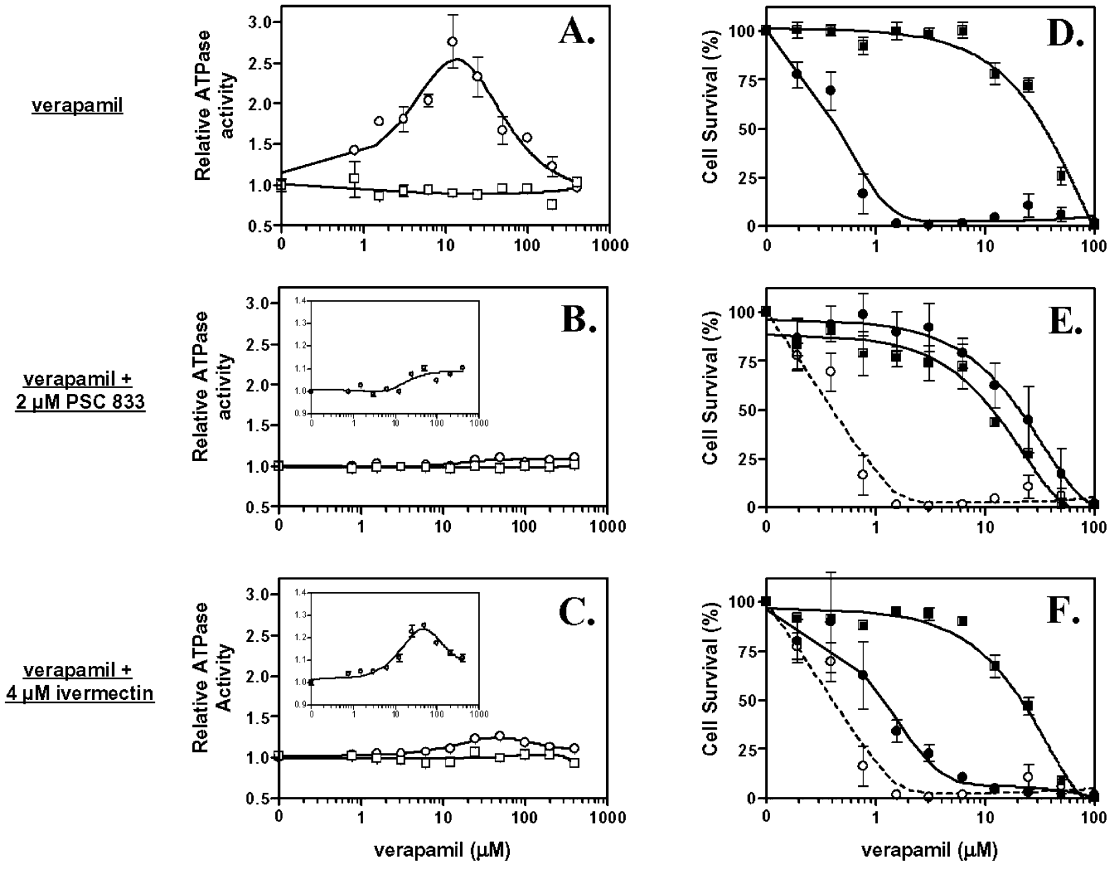

FIGURE 6: Effects of verapamil, PSC 833, and ivermectin on cell survival and P-gp1 ATPase in AUXB1 and CH^{R}C5. (A−C) ATPase activity of AUXB1 (white squares) and CH^{R}C5 (white circles) was measured using purified plasma membranes exposed to increasing concentrations of verapamil. In B and C, ATPase activity was measured with an additional pretreatment with 2 μM PSC 833 or 4 μM ivermectin. (D−F) Survival of AUXB1 (black squares) and CH^{R}C5 (black circles) exposed to increasing concentrations of verapamil was determined by staining colonies with methylene blue and quantified by spectrophotometry. In E and F, cell survival was determined with an additional pretreatment with 2 μM PSC 833 or 4 μM ivermectin. For a comparison, the dashed line in E and F shows the survival curve of CH^{R}C5 with verapamil alone from D.

10 μM in CH^{R}C5 cells. This concentration is comparable to the concentration of verapamil needed to induce apoptosis (Figures 1 and 2). From this we deduced that the effect of verapamil on ATPase activation may be linked to its ability to cause apoptosis. To test this, it was necessary to find inhibitors of verapamil-induced ATP hydrolysis. Cyclosporin A and PSC 833 are known inhibitors of P-gp1 ATPase. Unfortunately, cyclosporin A is also known to inhibit

apoptosis (*33*), leaving PSC 833. The ATPase activation by verapamil was almost completely reversed by 2 μM PSC 833 (Figure 6B). In addition, we found that ivermectin was an effective inhibitor of P-gp1 ATPase activity. Figure 6C shows that 4 μM ivermectin effectively inhibits P-gp1 ATPase stimulation by verapamil. Analysis of the ATPase inhibition with a smaller scale *Y*-axis shows that PSC 833 is a more effective inhibitor than ivermectin (inset graphs of Figure 6B,C). In fact, the characteristic biphasic ATPase activity produced by verapamil is still apparent with ivermectin.

To strengthen the correlation between apoptosis and P-gp1 ATPase, dose−response assays were conducted to see if CH^{R}C5 could be rescued from verapamil-induced apoptosis using ATPase inhibitors. As previously demonstrated, Figure 6D shows the effect of increasing amounts of verapamil on AUXB1 and CH^{R}C5. Cell survival was greatly reduced in CH^{R}C5 relative to AUXB1. The ability of 2 μM PSC 833 to modulate verapamil toxicity is shown in Figure 6E. The addition of PSC 833 almost completely inhibited the toxicity of verapamil, whereby the dose−response of AUXB1 and CH^{R}C5 was almost identical. The difference in the survival of CH^{R}C5 cells exposed to verapamil in the presence or in the absence of PSC 833 is illustrated by comparing the dashed line (no PSC 833) to the solid line (2 μM PSC 833). Ivermectin was also able to alter the toxicity caused by verapamil in CH^{R}C5 cells (Figure 6F). This effect is shown in comparing the survival of CH^{R}C5 cells without ivermectin (dashed line) and with 4 μM ivermectin. Interestingly, PSC 833 is a more potent ATPase inhibitor than ivermectin and reduced verapamil hypersensitivity more than ivermectin. These observations provided strong evidence that hypersensitivity to verapamil in MDR cells is directly associated with P-gp1 ATPase activation.

Production of Reactive Oxygen Species in CH^{R}C5 Cells by Verapamil. The correlation between ATP hydrolysis and apoptosis shown in Figure 6 is very interesting and likely to be a function of P-gp1 activity. Possibly, apoptosis was initiated by the high ATP demand from P-gp1. One consequence of an elevated energy demand would be an increase in ATP synthesis by oxidative phosphorylation in mitochondria. Several reactive oxygen species (ROS) are produced as byproducts of oxidative phosphorylation. To determine if ROS production is elevated in AUXB1 and CH^R-C5 cells exposed to verapamil, we measured production of the superoxide radical (O_2^-) through the reduction of MTT dye (*26*) (Figure 7A). A concentration of 10 μM verapamil was used to test ROS formation because it also induced high levels of ATPase activity as well as causing maximal killing of CH^{R}C5 cells. With the addition of 10 μM verapamil, the amount of superoxide in CH^{R}C5 cells was increased by almost 15% (Figure 7A). This indicates that verapamil selectively increases O_2^- production in CH^{R}C5 but not AUXB1 cells. In addition, we observed that ROS production in CH^{R}C5 decreased at higher concentrations of verapamil (25 and 75 μM). Our observations were not affected by the inadvertent transport of MTT dye by P-gp1 because a previous study established that MTT accumulation is not affected by the presence of P-gp1 (*34*). It was also determined that verapamil had no effect on MTT accumulation.

The MTT assay was not able to measure the effect of PSC 833 because it produced high background levels in our

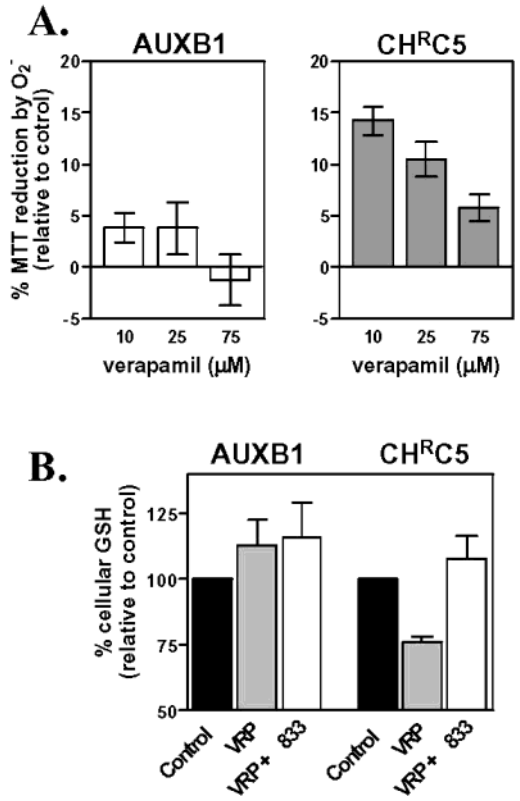

FIGURE 7: Superoxide production and GSH levels in AUXB1 and CH^{R}C5 exposed to verapamil and PSC 833. (A) MTT was used to measure superoxide (O_2^-) production in AUXB1 and CH^{R}C5 cells. Increasing amounts of verapamil (10, 25, and 75 μM) was added to cells. The graphs show the percent change in MTT reduction relative to untreated controls. (B) The total cellular GSH was determined in AUXB1 and CH^{R}C5 cells. Untreated control cells are displayed as black bars, cells treated with 10 μM verapamil (VRP) are in gray, and cells treated with both 10 μM verapamil and 2 μM PSC 833 (VRP + 833) are in white.

controls. Therefore, to determine the effect of PSC 833 on the oxidative state of cells, the total cellular glutathione (GSH) was measured (Figure 7B). GSH is a tripeptide that plays a major role as an antioxidant in the elimination of ROS. It is also a substrate for scavenging ROS through the GSH peroxidase and GSSG reductase (*35*). The results indicate that verapamil reduced GSH levels in CH^{R}C5 cells by almost 25%. PSC 833 was able to restore GSH levels to the same as control. No significant change in GSH was observed in AUXB1 with or without verapamil and PSC 833.

Reduction in Cellular ATP in CH^{R}C5 Cells by Verapamil. The ATPase activity of P-gp1 determined in the presence of verapamil (stimulator), PSC 833, and ivermectin (inhibitors) provided an indirect measure of cellular metabolism (Figure 6D−F). The two assays for ROS production also indicated the level of metabolic stress in CH^{R}C5 cells exposed to verapamil. By measuring the total cellular ATP levels in AUXB1 and CH^{R}C5 cells, we obtained a more direct view of the metabolic state of these cells when they are exposed to the above-mentioned drugs. The most striking result was observed in CH^{R}C5 cells exposed to 10 μM verapamil. The amount of ATP in CH^{R}C5 exposed to verapamil was less than half of the untreated control cells. This effect can be linked to the increased hydrolysis of cellular ATP by P-gp1 ATPase due to verapamil stimulation. When these cells were co-incubated with 2 μM PSC 833,

the level ATP in the cells returned to normal, probably as a result of ATPase inhibition. Both verapamil and PSC 833 had no significant effect on the amount of ATP in AUXB1 cells.

DISCUSSION

The phenomenon of hypersensitivity or collateral sensitivity to verapamil in MDR cells has been widely reported (*6*, *10*, *36*−*40*). To date, the mechanism and the role of P-gp1 in the development of hypersensitivity remain unclear. This study is the first attempt to resolve the mechanism of verapamil-induced P-gp1-mediated hypersensitivity in MDR cells. Specifically, our results show that verapamil hypersensitivity correlates with P-gp1 expression and its effects on P-gp1 ATPase activity. Moreover, verapamil-triggered apoptosis in P-gp1-positive CH^RC5 cells is not mediated though modulation of calcium levels or the expression of apoptosis related proteins (Bcl-2 or Bax). However, overexpression of Bcl-2 does reverse verapamil- and cisplatin-induced apoptosis in CH^RC5 cells. In addition, inhibition of P-gp1 ATPase by PSC 833 and ivermectin inhibits verapamil-induced apoptosis. These observations provide insight into the mechanism of verapamil collateral sensitivity.

An outstanding question relating to the role of P-gp1-associated hypersensitivity is the observation that not all P-gp1-expressing cells display hypersensitivity to verapamil. Our results suggest that other cellular changes, in addition to P-gp1 expression, appear to be required. Such changes include low redox capacity of MDR cells or high expression of pro-apoptotic proteins. Thus, tumor cells that overexpress P-gp1, together with high levels of anti-apoptotic proteins or high redox capacity, are unlikely to show verapamil hypersensitivity. These results are consistent with earlier observations that hypersensitivity to verapamil in resistant CHO cells is proportional to P-gp1 expression, but only at very high resistance levels (*10*). In that study, it was found that P-gp1 transfection of non-MDR AUXB1 and E29 cells (with ~9-fold colchicine resistance) did not produce verapamil hypersensitivity. Further selection of the transfectants with colchicine raised resistance by 200-fold, after which the cells developed verapamil hypersensitivity. In contrast, another study showed that NIH-3T3 cells develop verapamil hypersensitivity when transfected with P-gp1 cDNA (*37*). Our use of four CHO cell lines strengthens the observation that verapamil hypersensitivity is proportional to P-gp1 expression. The cell lines with higher P-gp1 expression displayed greater hypersensitivity to verapamil. The I10 cell line, a single-step MDR revertant from CH^RC5, emphasized the role of P-gp1 expression in this system because the only phenotypic difference between CH^RC5 and I10 is P-gp1 expression (*22*). The dose−response assay showed that hypersensitivity to verapamil was completely abrogated in I10 cells, solely as a result of reduced P-gp1 expression. This indicates that P-gp1 may be the sole factor mediating verapamil hypersensitivity in the CHO cells we used.

The present study demonstrates that activation of P-gp1 ATPase by verapamil induces excessive metabolic stress, leading to ROS-mediated apoptosis. The critical observation that allowed us to propose this mechanism was that CHO cells with high P-gp1 expression are more sensitive to low concentrations of verapamil (10 μM) than high concentrations (50 μM) (Figures 1 and 2). This biphasic trend is demonstrated in the 5-day clonal cell viability assay with AUXB1 and CH^RC5 cells. This effect is also evident in several other assays of cell survival. DNA laddering, Hoechst dye staining, and FACScan analysis served a dual role by showing hypersensitivity to low concentrations of verapamil, as well as indicating that the mechanism of cell death is apoptosis. Each assay consistently showed a biphasic trend in hypersensitivity to verapamil. The general trend with CH^RC5 is that survival decreases as verapamil concentrations reach approximately 10 μM. After this point, CH^RC5 survival begins to improve as verapamil concentrations increase to 50 μM. Finally, cell survival decreases to a fatal limit at about 100 μM verapamil. Interestingly, this unforeseen trend exposed a fascinating correlation between verapamil hypersensitivity and the activation of P-gp1 ATPase by verapamil.

Several mechanisms have been put forward to explain the hypersensitivity to verapamil. In one report, Stow and Warr (*40*) proposed that verapamil sensitivity occurs due to a mutation in P-gp1 during selection of MDR cells. The same group also put forward the possibility that high P-gp1 levels may destabilize the membrane, thereby affecting survival (*10*). We are proposing an alternate explanation based on P-gp1 ATPase activity.

It has been well documented that P-gp1 ATPase is particularly sensitive to activation by verapamil. Several drugs (e.g., vinblastine, paclitaxel, and verapamil) stimulate ATPase activity at low concentrations but inhibit the activity at higher concentrations (*12*, *14*, *20*, *41*). The similarity between ATPase activation and hypersensitivity is very striking. Not only were the biphasic curves for cell survival and ATPase activation very similar, but the verapamil concentration that caused maximum hypersensitivity (10 μM) also resulted in the highest level of ATPase activation. To further strengthen the link between P-pg1 ATPase and cell survival, we reasoned that, by inhibiting verapamil-induced ATPase activity, it would be possible to abrogate hypersensitivity to verapamil. Indeed, PSC 833 and ivermectin were able to reduce verapamil-induced ATPase stimulation as well as hypersensitivity in P-gp1 expressing cells. In addition, the more effective ATPase inhibitor, PSC 833, reduced collateral sensitivity to verapamil more effectively than ivermectin, the less potent ATPase inhibitor. The correlation between the degree of ATPase inhibition and modulation of cell survival provides convincing evidence that hypersensitivity to verapamil in P-gp1-expressing cells is directly linked to the stimulation of P-gp1 ATPase.

Interestingly, in addition to the well-known function of PSC 833 as an inhibitor of P-gp1-mediated MDR, several recent reports show that PSC 833 activates ceramide-dependent apoptosis (*42*−*45*). These observations favor PSC 833 as a cancer treatment because it inhibits P-gp1 as well as targeting MDR cells for apoptosis. In contrast, our results show for the first time that PSC 833 can prevent apoptosis by a pathway that is separate from its pro-apoptotic effects.

It was of interest to determine how P-gp1 ATPase stimulation by verapamil could cause apopsosis. ATP synthesis in eukaryotic cells is accomplished via glycolysis and mitochondrial oxidative phosphorylation. We believed that the second source provided ATP to P-gp1 ATPase for several reasons. A recent report shows that P-gp1 is dependent primarily on ATP produced in mitochondria by

F sub 1-ATPase and F sub 0-ATPase in the vinblastine-resistant leukaemic cell line, CEM/VLB$^{0.1}$ (*46*). Furthermore, it was shown that the P-gp1-expressing K/DAU$_{600}$ and CEM/VLB$_{100}$ cell lines have a more active electron transport chain (ETC) than their drug-sensitive parental cell lines, whereas glycolytic metabolism between resistant and sensitive cell lines remained consistent (*47*). One consequence of having ATP generated by the ETC in mitochondria, rather than glycolysis, is the generation of toxic ROS known to cause apoptosis (*48*, *49*).

The production of ATP through the coupling of electron transport and oxidative phosphorylation in mitochondria is normally very efficient (95−99%). When this process is uncoupled, electrons are lost and reduce oxygen to the superoxide radical (O_2^-). This radical can then go on to form other more destructive ROS such as hydrogen peroxide (H_2O_2) and eventually the highly reactive hydroxyl radical (OH$^\bullet$) (*50*). These can initiate apoptosis in a variety of ways. ROS cause apoptosis by reacting with, and damaging, biomolecules such as lipids and DNA (*51*−*53*). ROS-mediated apoptosis sometimes requires p53 activation, which does not appear to play a role in our system (Figure 3). ROS can also lead to mitochondrial permeability transition, which causes the release of apoptogenic factors such as cytochrome *c* and the apoptosis inducing factor (AIF), a process that is inhibited by Bcl-2 (*33*, *54*). Since we showed that verapamil hypersensitivity is inhibited by Bcl-2 (Figure 5), we believe that apoptosis in our system is mediated by a mitochondrial pathway.

We propose that cells with high P-gp1 expression exist in a state of heightened oxidative stress due to a highly active ETC. This situation is exaggerated when verapamil creates an even greater need for ATP by stimulating P-gp1 ATPase. We used two assays to show that hypersensitivity in P-gp1 expressing CH^{R}C5 cells was accompanied by an increase in ROS. When CH^{R}C5 cells were exposed to 10 μM verapamil, their O_2^- levels increased by approximately 15%, compared to 2% for AUXB1 (Figure 7A). Furthermore, increasing the concentration of verapamil above 10 μM resulted in decreased O_2^- levels. This trend is similar to the reduction in apoptosis and ATPase activity observed with the addition of increasing concentrations of verapamil. We also looked at the overall oxidative status of these cells by measuring the amount of GSH, a critical ROS scavenger in most cells (*35*). GSH levels were almost 25% lower in CH^{R}C5 exposed to verapamil compared to AUXB1 and untreated CH^{R}C5 cells. This indicated that the pool of available GSH had been reduced in CH^{R}C5, possibly due to higher than normal ROS production. These observations all point to greater metabolic stress in MDR cells exposed to verapamil.

Finally, in an attempt to gain a more direct measure of the metabolic state of MDR CH^{R}C5 cells exposed to 10 μM verapamil, we measured total cellular ATP relative to untreated controls. These observations confirmed that the stimulation of P-gp1 ATPase activity resulted in a reduction in the pool of cellular ATP by more than 50% (Figure 8). This effect has previously been observed in MDR human ovarian carcinoma cells, 2780AD, exposed to verpamil (*55*). This study found that 2780AD exposed to 8 μM verapamil had a reduction in the ATP:ADP ratio by about 50% relative to drug-sensitive parental cells, A2780. Moreover, we found that cellular ATP levels could be restored with 2 μM PSC 833. This evidence confirms that the metabolic state of MDR cells is directly altered by verapamil and PSC 833.

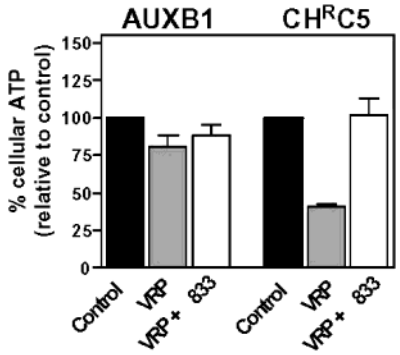

FIGURE 8: Total cellular ATP in AUXB1 and CHRC5 exposed to verapamil and PSC 833. The total cellular ATP levels were determined using the ATPlite luminescence ATP detection assay system. Untreated control cells are displayed as black bars, cells treated with 10 μM verapamil (VRP) are in gray, and cells treated with both 10 μM verapamil and 2 μM PSC 833 (VRP + 833) are in white.

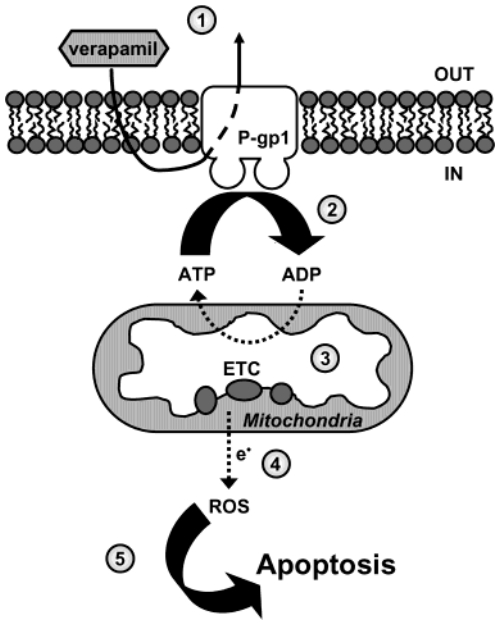

FIGURE 9: Proposed mechanism of verapamil collateral sensitivity in P-gp1 expressing cells. Verapamil crosses the cellular membrane and interacts with P-gp1, which transports verapamil back into the extracellular environment (1). The interaction with verapamil causes elevated levels of ATP hydrolysis by P-gp1 (2). This creates a high demand for ATP which is generated from oxidative phosphorylation in the mitochondria (3). As a result of the high ATP demand, electrons are lost from the electron transport chain (ETC), causing the production of higher than normal levels of ROS (4). The high concentration of ROS causes apoptosis by damaging lipids and DNA, or by initiating the cytocrome *c* apoptotic pathway (5).

This report presents evidence that verapamil hypersensitivity in MDR cells is associated with high levels of P-gp1 expression. In addition, we outlined a pathway in cells with high P-gp1 expression that leads to apoptosis. This pathway begins with an elevated ATP demand caused by verapamil, resulting in an overactive ETC which produces ROS and depletes cellular GSH, finally ending in apoptosis (see Figure 9). This new understanding of the mechanism of hypersensitivity in MDR cells could lead to a novel approach in the treatment of P-gp1-positive tumors. At present, the response

of P-gp1 ATPase to a diverse set of drugs has been characterized. Some of the less toxic drugs could be used to control the oxidative state of cancer cells, thereby targeting multidrug resistant tumors.

ACKNOWLEDGMENT

The authors thank Mrs. Zhi Liu and Ms. Francoise L'Heureux for their technical assistance in this study. Dr. G. J. Matlashewski (Department of Microbiology and Immunology, McGill University, Canada) generously provided the PG-13 CAT construct. We offer many thanks to our colleagues for their careful reading of this manuscript. This work is supported by a grant from the Canadian Institute of Health Research (CIHR) to E.G. M.L. is a recipient of the Max Stern Fellowship for McGill University.

SUPPORTING INFORMATION AVAILABLE

Figure showing the effects of deoxycorticosteroid and progesterone on cell survival and P-gp1 ATPase in AUXB1 and CHRC5. This material is available free of charge via the Internet at http://pubs.acs.org.

REFERENCES

1. Endicott, J. A., and Ling, V. (1989) *Annu. Rev. Biochem. 58*, 137−171.
2. Gottesman, M. M., and Pastan, I. (1993) *Annu. Rev. Biochem. 62*, 385−427.
3. Georges, E., Sharom, F. J., and Ling, V. (1990) *Adv. Pharmacol. 21*, 185−220.
4. Bech-Hansen, N. T., Till, J. E., and Ling, V. (1976) *J. Cell. Physiol. 88*, 23−31.
5. Cano-Gauci, D. F., and Riordan, J. R. (1987) *Biochem. Pharmacol. 36*, 2115−2123.
6. Warr, J. R., Anderson, M., and Fergusson, J. (1988) *Cancer Res. 48*, 4477−4483.
7. Barancik, M., Docolomansky, P., Slezak, J., and Breier, A. (1993) *Neoplasma 40*, 21−25.
8. Riehm, H., and Biedler, J. L. (1972) *Cancer Res. 32*, 1195−1200.
9. Tsuruo, T., Iida, H., Tsukagoshi, S., and Sakurai, Y. (1982) *Cancer Res. 42*, 4730−4733.
10. Warr, J. R., Quinn, D., Elend, M., and Fenton, J. A. (1995) *Cancer Lett. 98*, 115−120.
11. Naito, M., Hamada, H., and Tsuruo, T. (1988) *J. Biol. Chem. 263*, 11887−11891.
12. Shapiro, A. B., and Ling, V. (1994) *J. Biol. Chem. 269*, 3745−3754.
13. Ambudkar, S. V., Lelong, I. H., Zhang, J., and Cardarelli, C. (1998) *Methods Enzymol. 292*, 492−504.
14. Sharom, F. J., Yu, X., and Doige, C. A. (1993) *J. Biol. Chem. 268*, 24197−24202.
15. Shapiro, A. B., and Ling, V. (1995) *J. Biol. Chem. 270*, 16167−16175.
16. Sharom, F. J., DiDiodato, G., Yu, X., and Ashbourne, K. J. (1995) *J. Biol. Chem. 270*, 10334−10341.
17. Ruetz, S., and Gros, P. (1994) *Cell 77*, 1071−1081.
18. Ambudkar, S. V., Dey, S., Hrycyna, C. A., Ramachandra, M., Pastan, I., and Gottesman, M. M. (1999) *Annu. Rev. Pharmacol. Toxicol. 39*, 361−398.
19. Watanabe, T., Kokubu, N., Charnick, S. B., Naito, M., Tsuruo, T., and Cohen, D. (1997) *Br. J. Pharmacol. 122*, 241−248.
20. Litman, T., Zeuthen, T., Skovsgaard, T., and Stein, W. D. (1997) *Biochim. Biophys. Acta 1361*, 159−168.
21. Ling, V., and Thompson, L. H. (1974) *J. Cell. Physiol. 83*, 103−116.
22. Ling, V. (1975) *Can. J. Genet. Cytol. 17*, 503−515.
23. White, E., Cipriani, R., Sabbatini, P., and Denton, A. (1984) *J. Virol. 52*, 410−419.
24. Kern, S. E., Pietenpol, J. A., Thiagalingam, S., Seymour, A., Kinzler, K. W., and Vogelstein, B. (1992) *Science 256*, 827−830.
25. Laemmli, U. K. (1970) *Nature 227*, 680−685.
26. Towbin, H., Staehelin, T., and Gordon, J. (1979) *Proc. Natl. Acad. Sci. U.S.A. 76*, 4350−4354.
27. Burdon, R. H., Gill, V., and Rice-Evans, C. (1993) *Free Radical Res. Commun. 18*, 369−380.
28. Barry, M. A., Behnke, C. A., and Eastman, A. (1990) *Biochem. Pharmacol. 40*, 2353−2362.
29. Lee, S. C., Deutsch, C., and Beck, W. T. (1988) *Proc. Natl. Acad. Sci. U.S.A. 85*, 2019−2023.
30. Canman, C. E., and Kastan, M. B. (1995) *Semin. Cancer Biol. 6*, 17−25.
31. Baudier, J., Delphin, C., Grunwald, D., Khochbin, S., and Lawrence, J. J. (1992) *Proc. Natl. Acad. Sci. U.S.A. 89*, 11627−11631.
32. Massheimer, V., and de Boland, A. R. (1992) *Biochem. J. 281 (Pt. 2)*, 349−352.
33. Kroemer, G., Zamzami, N., and Susin, S. A. (1997) *Immunol. Today 18*, 44−51.
34. Marks, D. C., Belov, L., Davey, M. W., Davey, R. A., and Kidman, A. D. (1992) *Leuk. Res. 16*, 1165−1173.
35. Meister, A. (1988) *J. Biol. Chem. 263*, 17205−17208.
36. Cano-Gauci, D. F., Seibert, F. S., Safa, A. R., and Riordan, J. R. (1995) *Biochem. Biophys. Res. Commun. 209*, 497−505.
37. Croop, J. M., Guild, B. C., Gros, P., and Housman, D. E. (1987) *Cancer Res. 47*, 5982−5988.
38. Stow, M. W., and Warr, J. R. (1993) *FEBS Lett. 320*, 87−91.
39. Vickers, S. E., Stow, M. W., and Warr, J. R. (1993) *Cell. Biol. Int. 17*, 477−485.
40. Stow, M. W., and Warr, J. R. (1991) *Biochim. Biophys. Acta 1092*, 7−14.
41. al-Shawi, M. K., and Senior, A. E. (1993) *J. Biol. Chem. 268*, 4197−4206.
42. Cabot, M. C., Han, T. Y., and Giuliano, A. E. (1998) *FEBS Lett. 431*, 185−188.
43. Lehne, G., and Rugstad, H. E. (1998) *Br. J. Cancer 78*, 593−600.
44. Come, M. G., Bettaieb, A., Skladanowski, A., Larsen, A. K., and Laurent, G. (1999) *Int. J. Cancer 81*, 580−587.
45. Bezombes, C., Maestre, N., Laurent, G., Levade, T., Bettaieb, A., and Jaffrezou, J. P. (1998) *FASEB J. 12*, 101−109.
46. Jia, L., Allen, P. D., Macey, M. G., Grahn, M. F., Newland, A. C., and Kelsey, S. M. (1997) *Br. J. Haematol. 98*, 686−698.
47. Jia, L., Kelsey, S. M., Grahn, M. F., Jiang, X. R., and Newland, A. C. (1996) *Blood 87*, 2401−2410.
48. Lennon, S. V., Martin, S. J., and Cotter, T. G. (1991) *Cell Prolif. 24*, 203−214.
49. Chandra, J., Samali, A., and Orrenius, S. (2000) *Free Radical Biol. Med. 29*, 323−333.
50. Richter, C., Gogvadze, V., Laffranchi, R., Schlapbach, R., Schweizer, M., Suter, M., Walter, P., and Yaffee, M. (1995) *Biochim. Biophys. Acta 1271*, 67−74.
51. Maltzman, W., and Czyzyk, L. (1984) *Mol. Cell. Biol. 4*, 1689−1694.
52. Schreck, R., Albermann, K., and Baeuerle, P. A. (1992) *Free Radical Res. Commun. 17*, 221−237.
53. Christ, M., Luu, B., Mejia, J. E., Moosbrugger, I., and Bischoff, P. (1993) *Immunology 78*, 455−460.
54. Susin, S. A., Zamzami, N., Castedo, M., Hirsch, T., Marchetti, P., Macho, A., Daugas, E., Geuskens, M., and Kroemer, G. (1996) *J. Exp. Med. 184*, 1331−1341.
55. Broxterman, H. J., Pinedo, H. M., Schuurhuis, G. J., and Lankelma, J. (1990) *Br. J. Cancer 62*, 85−88.

BI034149+